Supplementary Material to "Novel magnetism of Ir^{5+} ($5d^4$) ions in the double perovskite Sr_2YIrO_6"

(Dated: December 20, 2013)

I. METHODS

Single crystals of Sr2YIrO6 and Sr2GdIrO6 were grown using a self-flux method from off-stoichiometric quantities of IrO2, SrCO3 and Y2O3 or Gd2O3, as described elsewhere [31, 32]. The diffraction data were refined using the full-matrix, least-squares SHELX-97 program [24]. Lattice parameters are shown in Table I

Compound	Structure	Space Group	$a(\AA)$	$b(\AA)$	$c(\AA)$	$\beta(\ ^\circ)$	IrO_6
Sr_2YIrO_6	Monoclinic	$P2_1/n$	5.7751	5.7919	8.1704	90.22	Flattened
Sr_2GdIrO_6	Cubic	Pn-3	8.2392				

TABLE I: Lattice Parameters for Sr_2YIrO_6 and Sr_2GdIrO_6.

II. PARALLEL STUDY OF GADOLINIUM COMPOUND

In the following we describe experimental details and results of a parallel study on Sr_2GdIrO_6. The structures of Sr_2YIrO_6 and Sr_2GdIrO_6 were determined using a Nonius Kappa CCD X-Ray Diffractometer with the sample temperature controlled using a nitrogen stream. The diffraction data were refined using the full-matrix, least-squares SHELX-97 program [24]. Chemical compositions of the single crystals were determined using energy dispersive X-ray analysis (EDX) (Hitachi/Oxford 3000). Magnetization, specific heat and electrical resistivity were measured using a Quantum Design MPMS 7 SQUID Magnetometer, and a Quantum Design Physical Property Measurement System (PPMS) with 14 T field capability. Specific heat and magnetic data in the milli-Kelvin range were obtained using a dilution refrigerator for the PPMS and an iQuantum insert for the MPMS, respectively.

A parallel study of Sr_2GdIrO_6 is also conducted for contrast and comparison. The cubic Sr_2GdIrO_6 is significantly less distorted than the monoclinic Sr_2YIrO_6 (Table 1), therefore no strong non-cubic crystal field is expected to compete with the SOI as it does in Sr_2YIrO_6. As shown in Supplemental Fig. 1, Sr_2GdIrO_6exhibits a robust ferromagnetic ordering among the $Gd^{3+}(4f^7)$ ions at $T_C = 2.3$ K, and a comparable Curie-Weiss temperature $\theta_{CW} = +1.2$ K. The inverse magnetic susceptibility $\Delta\chi^{-1}$ shown in Supplemental Fig. 1 a illustrates the sharply contrasting magnetic behavior of Sr_2GdIrO_6 and Sr_2YIrO_6, and provides additional evidence for strong quantum fluctuations signaled by the unusually large frustration parameter of 176.2 we observe in Sr_2YIrO_6. The isothermal magnetization $M(H)$ at 1.7 K exhibits a near saturation above 2 T and a saturation moment of $M_S \sim 7\ \mu_B$/f.u., which is consistent with the theoretical saturation moment for the $Gd^{3+}(4f^7)$ ions. As expected for a ferromagnet, application of magnetic fields readily broadens the magnetic anomaly in $C(T)$ and shifts the entropy to higher temperatures, as shown in Supplemental Fig. 4c. In contrast, Sr_2YIrO_6 exhibits a vastly different response to magnetic fields: both $C(T)$ and $S(T)$ are drastically enhanced at $\mu_0 H = 1$ T before being suppressed at higher fields (Fig. 1), implying weak magnetic order among partially developed moments. Furthermore, there is no evidence for any magnetic ordering due to the Ir^{5+} ions in Sr_2GdIrO_6. A recent electronic structure study [28] reveals that both the magnetic and orbital moments at the Ir sites vanish when the SOC is included in the calculations. Indeed, in the absence of a strong non-cubic field, the SOC prevails and renders the Ir^{5+} ions nonmagnetic, as expected in the strong SOC limit.

The presence of the addition interactions between Ir-5d and Gd-4f electrons also renders a less insulating state in Sr_2GdIrO_6, as shown in Supplemental Fig. 2. Activation law fits to the data yield the activation gap 490 meV and 272 meV for $Sr_2YIrO_6$and Sr_2GdIrO_6, respectively.

III. DETAILS OF THE 4-PARTICLE CALCULATIONS

In this part of the supplemental material we give details of the 4-particle states in various regimes of parameters. We start with the interaction Hamiltonian of Eq. (2) of the main manuscript:

$$H_H = -J_H\left(\mathbf{S}_{tot}\right)^2 + J_H T^\dagger T \tag{1}$$

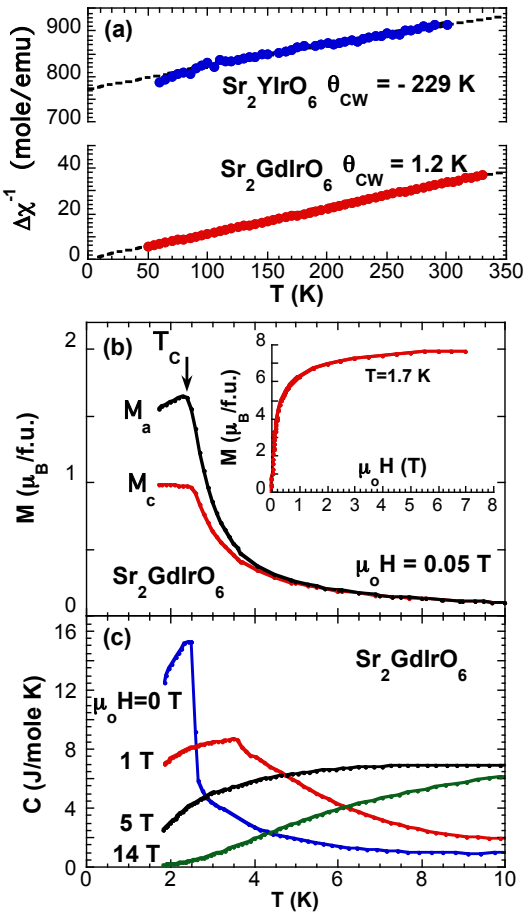

FIG. 1: A comparison of the inverse magnetic susceptibility $\Delta\chi^{-1}$ at $\mu_0 H = 0.1$ T for 50 K $< T <$ 350 K between Sr_2YIrO_6 and Sr_2GdIrO_6. Note the drastic difference in the Curie-Weiss temperature θ_{CW} between the two double perovskites. Magnetic and thermal properties of Sr_2GdIrO_6: (b) the low-temperature magnetization $M(T)$ at $\mu_0 H = 0.1$ T for the a- and c-axis; Inset: the isothermal magnetization $M(H)$ at $T = 1.7$ K; and (c) the specific heat $C(T)$ at $\mu_0 H = 0$, 1, 5, and 14 T.

where $\mathbf{S}_{tot}$ is the total spin of the 4 particles, and T is the "Cooper pair" operator. When angular momenta are quantized in the z-direction, one can write $T = \sum_{m=0,\pm1}(-1)^m c_{-m\downarrow} c_{m\uparrow}$. This interaction commutes with all components of $\mathbf{L}$ and $\mathbf{S}$ separately. The eigenstates can be conveniently expressed in terms of the quantum numbers $L,\ M_L,\ S,\ M_S$, where $L,\ S$ are the total orbital and spin angular momenta of the 4-particle state and $M_L,\ M_S$ are their z-projections.

It turns out to be convenient to take the fully filled 6-particle state $|\Omega\rangle$ as the reference state, and consider 2-hole states (which are completely equivalent to the 4-particle states). For two holes with $l = 1$ and $s = 1/2$ each, the possible states with the proper antisymmetry are $L = S = 0$ (a single state), $L = S = 1$ (9-fold degenerate), and $L = 2,\ S = 0$ (5-fold degenerate). It is easy to check that the singlet has energy $4J_H$, the $S = 0$ quintuplet has energy J_H, while the 9-fold degenerate manifold has energy $-J_H$.

Let us make the assumption that $J_H \gg \lambda, \Delta$ is the largest energy scale in the problem. This assumption makes it very easy to analytically determine all the energies. It also turns out that the results derived in this regime are quite accurate even in the physical regime, where J_H is larger than, but not much larger than $\lambda,\ \Delta$. The figures show results obtained by keeping all 15 4-particle states, while the analytical analysis will hold for the lowest 9.

For $J_H \gg \lambda, \Delta$, we need consider only the $L = S = 1$ multiplet. We can list the states (with labels M_L, M_S) in

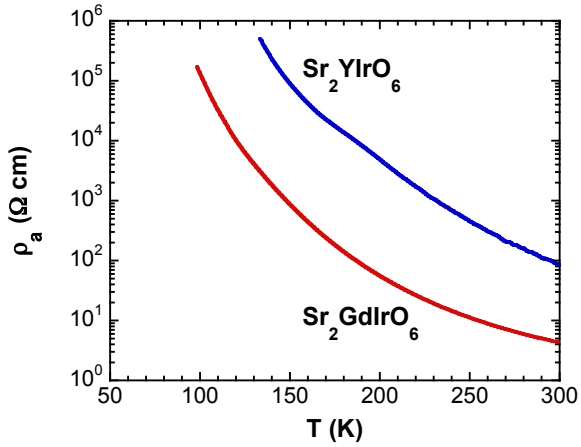

FIG. 2: The temperature dependence of electrical resistivity for Sr_2YIrO_6 and Sr_2GdIrO_6.

second-quantization as follows:

$$|-1,-1\rangle = c_{0\uparrow}c_{1\uparrow}|\Omega\rangle \qquad |0,-1\rangle = c_{1\uparrow}c_{-1\uparrow}|\Omega\rangle \qquad |1,-1\rangle = -c_{0\uparrow}c_{-1\uparrow}|\Omega\rangle \tag{2}$$

$$|-1,0\rangle = -\frac{c_{0\uparrow}c_{1\downarrow}+c_{0,\downarrow}c_{1\uparrow}}{\sqrt{2}}|\Omega\rangle \qquad |0,0\rangle = -\frac{c_{1\uparrow}c_{-1\downarrow}+c_{1\downarrow}c_{-1\uparrow}}{\sqrt{2}}\Omega\rangle \qquad |1,0\rangle = \frac{c_{0\uparrow}c_{-1\downarrow}+c_{0\downarrow}c_{-1\uparrow}}{\sqrt{2}}|\Omega\rangle \tag{3}$$

$$|-1,1\rangle = c_{0\downarrow}c_{1\downarrow}|\Omega\rangle \qquad |0,1\rangle = c_{1\downarrow}c_{-1\downarrow}|\Omega\rangle \qquad |1,1\rangle = -c_{0\downarrow}c_{-1\downarrow}|\Omega\rangle \tag{4}$$

Let us now examine the spin-orbit and tetragonal distortion operators. They are

$$H_{SO} = -\lambda\left(\tfrac{1}{2}(n_{1\uparrow}-n_{1\downarrow}-n_{-1\uparrow}+n_{-1\downarrow})+\frac{1}{\sqrt{2}}(c^\dagger_{1\downarrow}c_{0\uparrow}+c^\dagger_{0\downarrow}c_{-1\uparrow}+c^\dagger_{0\uparrow}c_{1\downarrow}+c^\dagger_{-1\uparrow}c_{0\downarrow})\right) \tag{5}$$

$$H_\Delta = -\Delta N_{tot}+\Delta(n_{0\uparrow}+n_{0\downarrow}) \tag{6}$$

It is clear that H_Δ is completely diagonal in the basis we have constructed, while H_{SO} conserves $M_L+M_S=M_J$. Clearly, the states $|-1,-1\rangle,\ |1,1\rangle$ do not couple to any others, and are therefore eigenstates. Their energy is $E_{1,1}=E_{-1,-1}=-J_H-3\Delta+\lambda/2$. Next, there are two two-dimensional subspaces, one formed by $|M_L,M_S\rangle=|-1,0\rangle,\ |0,-1\rangle$ with $M_J=-1$, and the other formed by the states $|0,1\rangle,\ |1,0\rangle$ with $M_J=1$. Their energetics will be identical by time-reversal symmetry, so we examine only the first. In this subspace $H_{SO}+H_\Delta$ is the two-dimensional matrix

$$\begin{pmatrix} -3\Delta & \frac{\lambda}{2} \\ \frac{\lambda}{2} & -2\Delta \end{pmatrix} \tag{7}$$

The eigenvalues are $-\frac{5}{2}\Delta\pm\frac{1}{2}\sqrt{\Delta^2+\lambda^2}$.

Finally, the three states $|-1,1\rangle,\ |0,0\rangle,\ |1,-1\rangle$ in the $M_J=0$ subspace are all connected. In this subspace $H_{SO}+H_\Delta$ forms the matrix

$$\begin{pmatrix} -3\Delta-\frac{\lambda}{2} & \frac{\lambda}{2} & 0 \\ \frac{\lambda}{2} & -2\Delta & \frac{\lambda}{2} \\ 0 & \frac{\lambda}{2} & -3\Delta-\frac{\lambda}{2} \end{pmatrix} \tag{8}$$

We notice that the state $|0,0\rangle$ couples only to the symmetric combination $(|-1,1\rangle+|1,-1\rangle)/\sqrt{2}$, and the antisymmetric combination decouples. This leads to a two-dimensional problem which can be easily solved. The energies in the $M_J=0$ subspace are $-3\Delta-\frac{\lambda}{2}$ (the antisymmetric combination), and $-\left(\frac{5\Delta}{2}+\frac{\lambda}{4}\right)\pm\frac{1}{2}\sqrt{\left(\Delta+\frac{\lambda}{2}\right)^2+2\lambda^2}$.

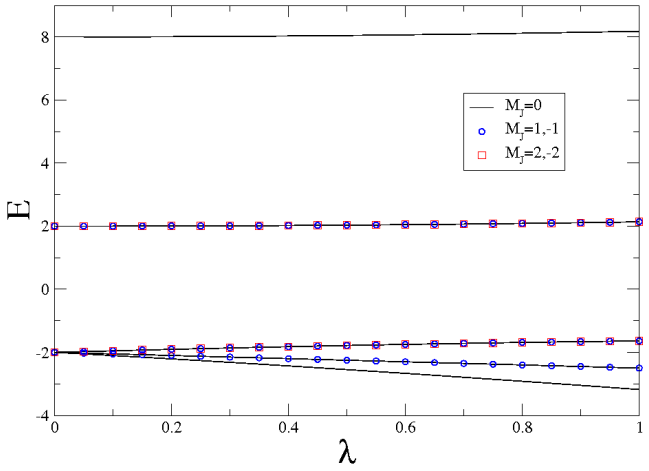

FIG. 3: All the 4-particle states for $J_H = 2$ as a function of λ. The black lines represent states with $M_J = 0$, the blue circles represent $M_J = \pm 1$ and the red squares represent $M_J = \pm 2$. The lowest level of $M_J = 0$ is a singlet. Each level shown for $M_J = \pm 1,\ \pm 2$ is doubly degenerate by time-reversal symmetry. So the ground state is always a singlet, and is separated from the next triplet manifold by $\frac{\lambda}{2}$.

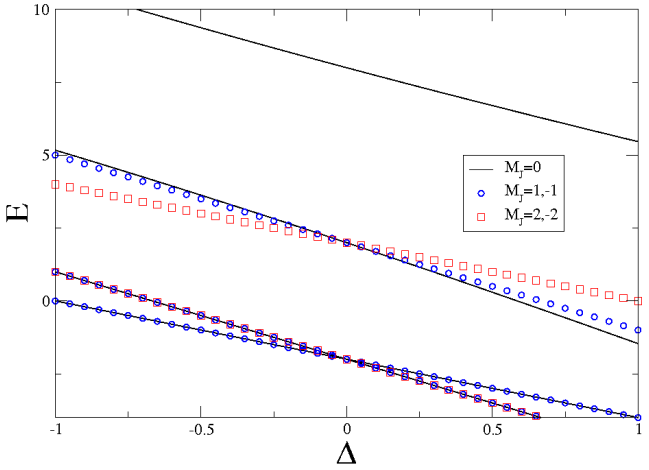

FIG. 4: All the 4-particle states for $J_H = 2$ as a function of Δ. The black lines represent states with $M_J = 0$, the blue circles represent $M_J = \pm 1$ and the red squares represent $M_J = \pm 2$. The lowest level of $M_J = 0$ is a singlet for $\Delta < 0$ and a doublet for $\Delta > 0$. Each level shown for $M_J = \pm 1,\ \pm 2$ is doubly degenerate by time-reversal symmetry. So for $\Delta > 0$ the ground state is 6-fold degenerate while for $\Delta < 0$ it is 3-fold degenerate.

Now we are in a position to take various limits. First consider the $\Delta = 0$ limit. In this limit, there is a single state at an energy $-\lambda$ (coming from the $-$ sign in the $M_J = 0$ sector), a 5-fold degenerate state at an energy $-\frac{\lambda}{2}$, and a 3-fold degenerate state at $\frac{\lambda}{2}$. Thus, there is a gap of $\frac{\lambda}{2}$ between the singlet and the next manifold. This state of affairs is shown in Fig. 3.

Let us consider the opposite limit $\lambda = 0$. Now there are 6 states at -3Δ and 3 states at -2Δ. For $\Delta = -|\Delta| < 0$, which is the regime of interest to us, the ground state is 3-fold degenerate.

Now if we turn on λ, the lowest state comes from the $M_J = 0$ sector and has the energy $-\left(\frac{5\Delta}{2} + \frac{\lambda}{4}\right) - \frac{1}{2}\sqrt{\left(\Delta + \frac{\lambda}{2}\right)^2 + 2\lambda^2}$, while above it is a doublet (arising from the $M_J = \pm 1$ sectors) with energy $-\frac{5}{2}\Delta - \frac{1}{2}\sqrt{\Delta^2 + \lambda^2}$.

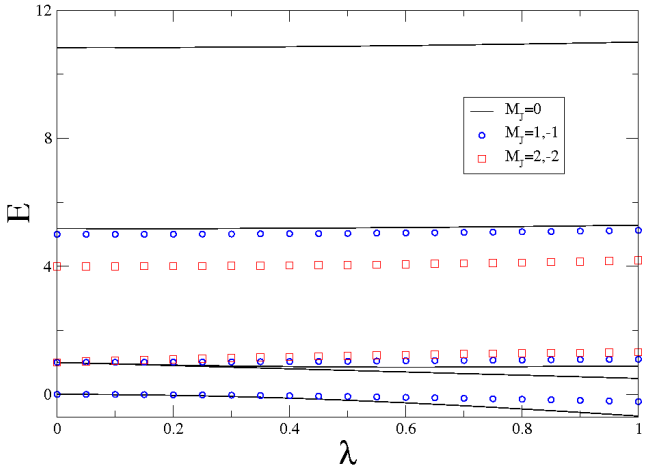

FIG. 5: The energies of 4-particle states as a function of λ for $J_H = 2$, $\Delta = -1$. The black lines represent states with $M_J = 0$, the blue circles represent $M_J = \pm 1$ and the red squares represent $M_J = \pm 2$. The lowest $M_J = 0$ state is a singlet, and the next manifold is a doublet arising from $M_J = \pm 1$. We see that the gap between the two remains small all the way to $\lambda = |\Delta|$.

For $\lambda \ll \Delta$ the energy difference is $\delta = \frac{\lambda^2}{4|\Delta|}$. In fact, this approximation works quite well almost all the way to $\lambda = |\Delta|$. We see in this case a small gap between the singlet ground state and a doublet.